Indonesian Journal of Electrical Engineering and Informatics (IJEEI)
Vol. 9, No. 3, September 2021, pp. 647~661
ISSN: 2089-3272, DOI: 10.52549/ijeei.v9i3.2481

Design of FIR digital filters using Semi-ellipse window

Henry N. Uzo[1], Ogbonna U. Oparaku[2], Vincent C. Chijindu[3]
[1]Department of Electrical R&D, Scientific Equipment Development Institute, Enugu - Nigeria
[2,3]Department of Electronic Engineering, University of Nigeria, Nsukka - Nigeria

Article Info

Article history:

Received May 17, 2020
Revised Aug 30, 2021
Accepted Sep 17, 2021

Keywords:

Bartlett window
Fixed window
Nonrecursive digital filter
Ripple ratio
Semi-ellipse

ABSTRACT

A fixed window function which is similar in shape to a semi-ellipse is proposed. The semi–ellipse which has its major axis to be equal to the window length and the minor axis at unity produced about 4.2 dB lower ripple ratio than the rectangular window. The proposed window function is derived from the equation of an ellipse in the explicit and parametric forms. First of all, the spectral characteristic of the proposed window is studied in terms of spectral parameters and compared with other fixed windows like Rectangular, Bartlett, Hann, Hamming and Blackman windows. The window simulation results reveal that the proposed window produced comparable spectral characteristic with existing standard fixed windows. Secondly, the paper presents the application of the proposed window in a digital filter design. The filter analysis comparison results with other fixed windows namely Bartlett, Von Hann, Hamming, and Kaiser window, an adjustable window, confirm that filter design with the proposed window exhibits good spectral characteristic, and can be used to design better filter than the Bartlett window using less than half the Bartlett's filter length for a fixed transition width. The similicity of its coefficients formulation and design algorithm makes it a good choice for digital filter design applications.

Corresponding Author:

Henry N. Uzo,
Department of Electrical R&D,
Scientific Equipment Development Institute (SEDI),
P.O. Box 3205, Enugu – Nigeria.
Email: nhenryuzo@gmail.com

1. INTRODUCTION

Digital filters are essential part of digital signal processing (DSP). DSP growth over the years is because of the astonishing performance of the digital filters. The ideal approach to the design of discrete-time infinite impulse responses filters involves the transformation of a continuous-time filter into a discrete-time filters meeting some prescribed specifications [1, 2]. Discrete-time filters can be classified on the basis of the duration of their impulse response either as infinite impulse response (recursive) filters or as finite impulse response (nonrecursive) filters. The finite impulse response (FIR) filters are frequently used in digital filter design due to the fact that they are stable, and they have linear phase characteristics. Its major drawback is complexity because it requires relatively large filter length compared to infinite impulse response (IIR) filter in satisfying prescribed filter characteristics [2-4].

FIR filters design can be achieved using different techniques and most of them are based on ideal filter approximation. These techniques include window technique based on Fourier series, frequency sampling technique, and numerical method [2-4]. The simplest technique of FIR filter design is the window method. A window is an array consisting of coefficients that meet proposed filter requirements [2, 3]. The impulse response of an ideal filter is infinite in nature so truncating at some point say M at both negative and positive sides of the filter impulse response (see Figure 1) yields a symmetrical FIR filter of length, $N = 2M + 1$. The effect of making the infinite-duration impulse response to be finite gives rise to the Gibbs phenomenon [4-6] – ripples in the passband and attenuation in the stopband as shown in Figure 2.

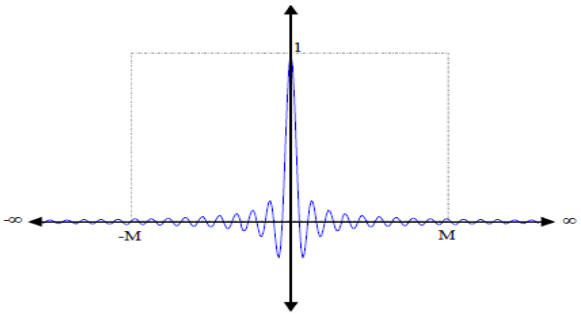

Figure 1. The impulse response of an ideal filter

The truncation done in Figure 1 is achieved using a sharp-edge window which is rectangular in shape. However, increasing the filter length, N increases the frequency of the oscillation, but does not reduce the amplitude of the ripples in the passband and stopband rather the discontinuity is significant no matter how long the filter length is made as shown in Figure 2.

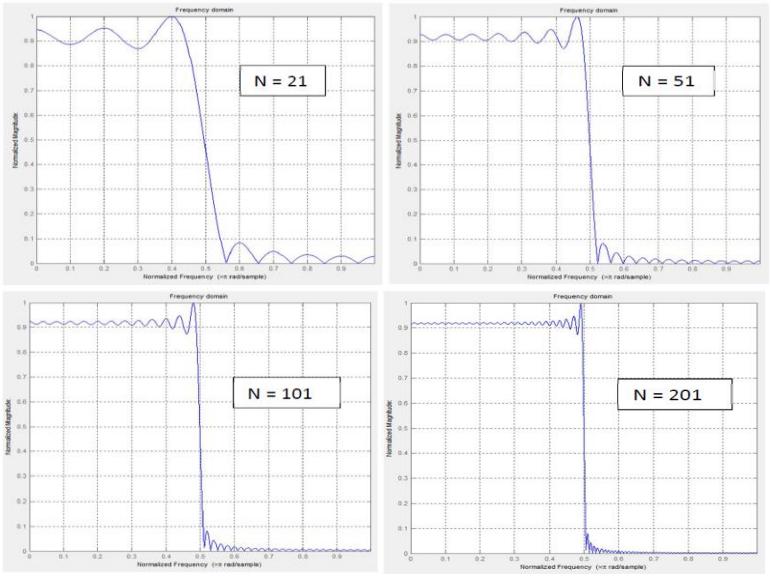

Figure 2. The Gibbs phenomenon

Fortunately, the application of window functions which have tapering edge improves this situation. Figure 3 depicts the rectangular (sharp-edge) and nonrectangular (tapering edge) window function. Therefore, multiplying the ideal filter impulse response, $h_{id}(n)$, by a window function w(n), results in the windowed FIR filter, h(n). The FIR digital filter design using windows is discussed in Section 2.4.

The idea is to reduce the abruptness of the truncated ends and thereby improve the frequency response. The desired objectives of windowed FIR filter design include:

- Minimize the ripples in the passband to achieve good flat passband.
- Minimize the ripples in the stopband to achieve good stopband attenuation.
- Shrink the main-lobe width to realize a narrow transition band width (i.e. fast roll-off).
- The length of the filter should be made as few as possible to decrease complexity.

Several different windows are available, and a list of window functions could be found in [7]. Windows can be categorized as fixed or adjustable window depending on the number of independent window parameters in their function [8]. A fixed window has only one independent parameter – the window length.The window function proposed in this work is fixed. Some fixed windows exist in literature namely Rectangular, Triangular (aka Bartlett window), Hamming, Von Hann and Blackman windows [1-4, 6, 7]. An adjustable window has two or more independent parameters which include the window length. A variety of adjustable window functions also exist in literature like the Kaiser window [9], ultraspherical window[10] and Dolph Chebychev window[11]. The independent parameters are used to control the window characteristics.

Figure 3 depicts the rectangular (sharp-edge) and nonrectangular (tapering edge) window function.

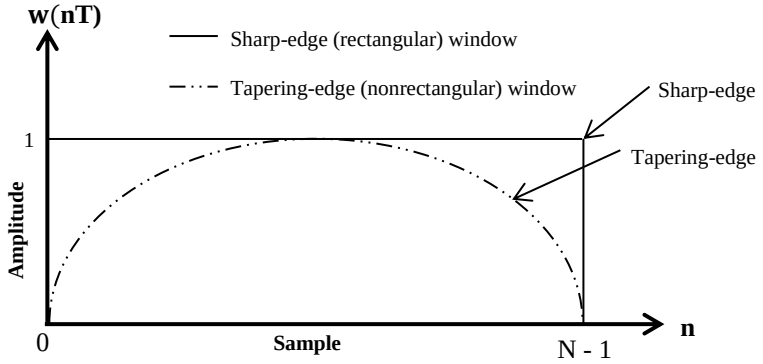

Figure 3. The sharp-edge rectangular window gives rise to Gibbs oscillation while the tapering-edge windows reduce the problem

Besides, window functions can be combined to produce a hybrid window function with improved spectral characteristics for various filter applications. Some of these hybrid windows include Bartlett-Hann [3, 7] and Blackman-Harris [12]. Most window functions proposed lately fall into this category; the authors in [13] developed a hybrid of Blackman window and Kaiser window; the authors in [14] combined tangent hyperbolic function and a weighted cosine series, while in [15] they combined Blackman Window and Lanczos Window.

In this paper, an efficient formulation for generating the coefficients of the Semi-ellipse window is proposed and its application for the design of FIR digital filters that would satisfy prescribed specifications is demonstrated. The paper is organized as follows. Section 2, first of all, introduces the fixed window functions and the basic parameters that classify their spectral characteristic; secondly, an efficient formulation for generating the coefficients of the Semi-ellipse window is described; thirdly, the parameters that describe the proposed window are illustrated; lastly, the proposed window is used in the design of FIR digital filters with other windows which illustrates the use of its design algorithm with some examples. Section 3 provides the results and discussion while Section 4 gives the conclusion.

2. PROPOSED RESEARCH METHOD

2.1. Window spectral characteristics

A typical window function diagram is shown in Figure 4(a) which is noncausal because it is zero-centered. A causal window function can be obtained by shifting the window function by half its length, hence making the window to be zero for negative time (see Figure 4(b)). The shift property of the Fourier transform that makes the impulse response to be symmetrical about $(N-1)/2$ has introduced a linear phase form [2].

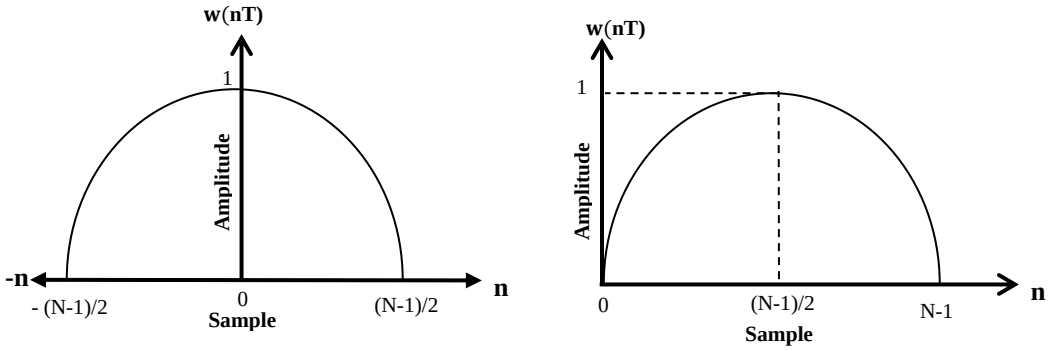

Figure 4. The noncausal (a) and causal (b) window functions

The most commonly used window functions are defined in their causal forms using the following equations [2-4, 6, 7]:

- **Rectangular window**

$$w_{rec}(n) = 1, \quad \begin{cases} 0 \le n \le N-1 \\ 0 \quad otherwise \end{cases} \tag{1}$$

- **Triangular (Bartlett) window**

$$w_{tri}(n) = \begin{cases} \frac{2n}{N-1}; & 0 \le n \le \frac{N-1}{2} \\ 2 - \frac{2n}{N-1}; & \frac{N-1}{2} \le n \le N-1 \\ 0; & otherwise \end{cases} \quad (2)$$

- **Von Hann window**

$$w_{han}(n) = 0.5 - 0.5\cos\left(\frac{2\pi n}{N-1}\right), \begin{cases} 0 \le n \le N-1 \\ 0 \quad otherwise \end{cases} \quad (3)$$

- **Hamming window**

$$w_{ham}(n) = 0.54 - 0.46\cos\left(\frac{2\pi n}{N-1}\right), \begin{cases} 0 \le n \le N-1 \\ 0 \quad otherwise \end{cases} \quad (4)$$

- **Blackman window**

$$w_{bl}(n) = 0.42 - 0.5\cos\left(\frac{2\pi n}{N-1}\right) + 0.08\cos\left(\frac{4\pi n}{N-1}\right), \begin{cases} 0 \le n \le N-1 \\ 0 \quad otherwise \end{cases} \quad (5)$$

- **Kaiser window**

Unlike all the fixed windows mentioned above, the Kaiser window is an adjustable window function. The window is proposed by Kaiser [9], and it is used widely. The Kaiser window function is given by:

$$w_{kai}(n) = \frac{I_0\left(\beta.\sqrt{1-\left(\frac{n-\alpha}{\alpha}\right)^2}\right)}{I_0(\beta)}; \begin{cases} 0 \le n \le N-1 \\ 0 \quad otherwise \end{cases} \quad (6)$$

where $\propto = \frac{N-1}{2}$ and I_0 is a modified zero order Bessel function of the first kind.

$$\text{and, } \beta = \begin{cases} 0.1102(A_s - 8.7); & A_s > 50 \\ 0.5842(A_s - 21)^{0.4} + 0.07886(A_s - 21); & 21 < A_s < 50 \\ 0; & A_s < 21 \end{cases} \quad (7)$$

where A_s = minimum stopband attenuation

The filter length, N can be determined by selecting the lowest odd value of N that would satisfy the inequality:

$$N \ge \frac{\omega_{samp} D}{\Delta\omega} + 1 \quad (8)$$

Parameter D is determined using the expression:

$$D = \begin{cases} 0.9222; & A_s \le 21 \\ \frac{A_s - 7.95}{14.36}; & A_s > 21 \end{cases} \quad (9)$$

Where ω_{samp} is the normalized sampling frequency and $\Delta\omega$ is the transition width.

However, windows are analysed in the frequency domain in order to compare and classify them in term of their spectral characteristics. The frequency spectrum of a window can be obtained as given by [1]

$$W(e^{j\omega T}) = e^{-j\omega(N-1)T/2} W_0(e^{j\omega T}) \quad (10)$$

Where $W_0(e^{j\omega T})$ is the amplitude function, N is the window length, and T is the interval between samples and T is taken to be 1 second throughout this paper for simplicity, hence T = 1.

The normalized amplitude spectrum of a typical window is shown in Figure 5 [16].

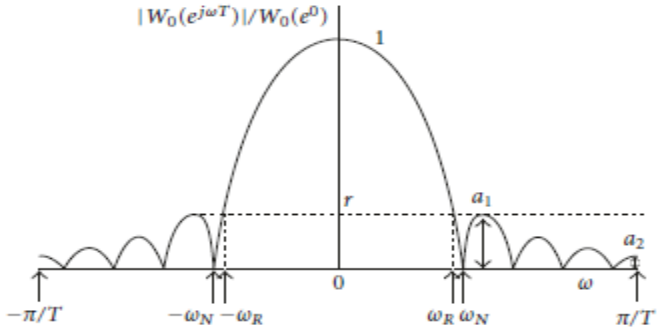

Figure 5. Normalized amplitude spectrum of a typical window

Figure 5 depicts the two basic parameters that characterize a window in the frequency domain. They are the main-lobe width, W_{ML} and the ripple ratio, r also refer to as the maximum side-lobe amplitude. The main-lobe width, W_{ML} is the bandwidth between the first negative and first positive zero crossing which is equal to $2W_R$, and ripple ratio, r is the maximum side-lobe amplitude, $A_{SL_{max}}$ divided by the main-lobe amplitude, A_{ML}. The ripple ratio is given as expressed in (11) [1].

$$r = \left(\frac{A_{SL_{max}}}{A_{ML}}\right) 100\% \quad \text{or} \quad R = 20 \log\left(\frac{A_{SL_{max}}}{A_{ML}}\right) \text{dB} \tag{11}$$

2.2. The proposed Semi-ellipse window

In this section, we derived the proposed window function using the equation of an ellipse in two different forms that yielded equivalent results. These methods are illustrated as in [17]:

- Equation of an ellipse in explicit form
- Equation of an ellipse in parametric form

2.2.1. Equation of an ellipse in explicit form

The equation of an ellipse in explicit form (12) with reference to Figure 6 showing an ellipse inscribed in the rectangle AEFD.

$$\frac{(n+h)^2}{a^2} + \frac{(w+k)^2}{b^2} = 1 \tag{12}$$

Where *a* is the radius of the major axis, and *b* is the radius of the minor axis while its centre coordinate is h on n-axis and k on w-axis

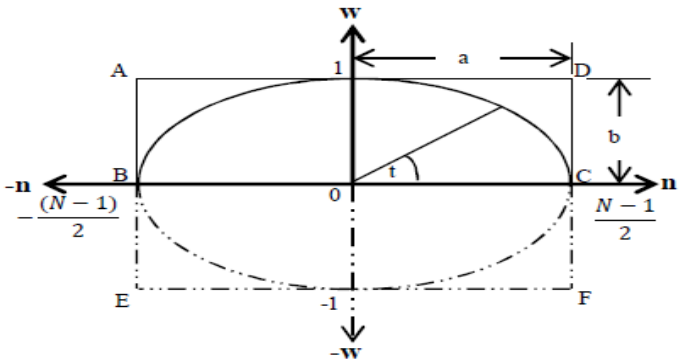

Figure 6. An ellipse with radius of the major axis, a = (N-1)/2 and the radius of the minor axis, b = 1 having its center at the origin

Referring to Figure 6, $a = \frac{N-1}{2}$ (13)

and b = 1 (14)

also, the ellipse centre coordinate, (h, k) = (0, 0)

Substituting (13) and (14) into (12), with centre of coordinate of the ellipse as (0, 0) yields:

$$\frac{4n^2}{(N-1)^2} + w^2 = 1 \tag{15}$$

The last equation can also be rewritten as:

$$w = \pm\sqrt{1 - \frac{4n^2}{(N-1)^2}} \quad (16)$$

Considering the positive semi-ellipse (see Figure 6), inscribed in rectangle, ABCD (the rectangle with the solid line), the proposed Semi-Ellipse window is given by:

$$w_{se}(n) = \sqrt{1 - \frac{4n^2}{(N-1)^2}}\ ; \quad \begin{cases} -\frac{N-1}{2} \le n \le \frac{N-1}{2} \\ 0 \quad otherwise \end{cases} \quad (17)$$

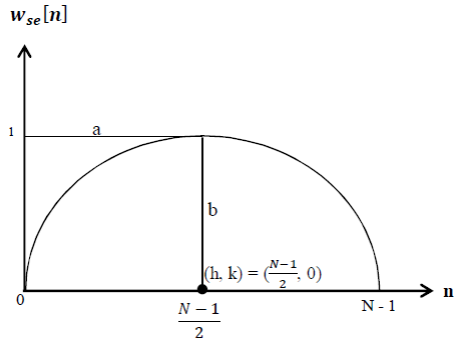

Figure 7. Proposed semi-ellipse window shifted to run from 0 to (N-1)

The proposed window functions when shifted to the right by (N-1)/2 to runs from 0 to (N-1), using only positive indexes, is shown in Figure 7. Thus, the causal form of the proposed Semi-ellipse window is defined as:

$$\mathrm{w_{se}(n)}_{causal} = \mathrm{w_{se}}\left(\mathrm{n} - (\tfrac{N-1}{2})\right) = \tfrac{2}{(N-1)}\sqrt{(N-1)n - n^2};\ \begin{cases} 0 \le n \le N-1 \\ 0 \quad otherwise \end{cases} \quad (18)$$

2.2.2. Equation of an ellipse in parametric form

The general parametric equations of an ellipse with centre at coordinate (h, k) are given by:

$$n = h + acost \quad (19)$$

And,

$$w = k + bsint \quad (20)$$

where the parameter t is an angle $0 \le t \le 2\pi$ (see Figure 6). Equation (19) can also be rewritten as

$$t = \arccos(\tfrac{n-h}{a}) \quad (21)$$

Substituting (21) into (20) yields,

$$w = k + b\sin(\arccos(\tfrac{n-h}{a})) \quad (22)$$

Considering the semi-ellipse plotted in Figure 7 and replacing all the variables appropriately, (22) yields:

$$w = \sin(\arccos(\tfrac{2n}{N-1} - 1)) \quad (23)$$

Therefore, the equivalent function of the proposed semi-ellipse window of (18) in parametric form is given by:

$$w_{se}(n) = \sin\left(arccos\ (\tfrac{2n}{N-1} - 1)\right); \begin{cases} 0 \le n \le N-1 \\ 0 \quad otherwise \end{cases} \quad (24)$$

2.3. The proposed window spectral characteristics

In this section, the window spectrum of the proposed Semi-ellipse window is observed and examined to determine its spectral characteristics in terms of the main-lobe width and the ripple ratio. Generally, it is observed that the main-lobe width of window functions decreases as the window length increases [1-4]. Hence, N is proportional to $1/W_{ML}$, we can control the main-lobe width using the length of the window. The proposed Semi-ellipse window length, N is plotted against the reciprocal of its main-lobe width, W_{MLse} as shown in Figure 8. The result reveals that the main-lobe width of the proposed Semi-ellipse W_{MLse} window assumes a value that can be determined as given by:

$$W_{ML_{se}} \approx \frac{5}{N}\ (\mathrm{x}\pi\ \mathrm{rad/sample}) \quad (25)$$

where $W_{ML_{se}}$ is the proposed Semi-ellipse main-lobe width and N is the window length

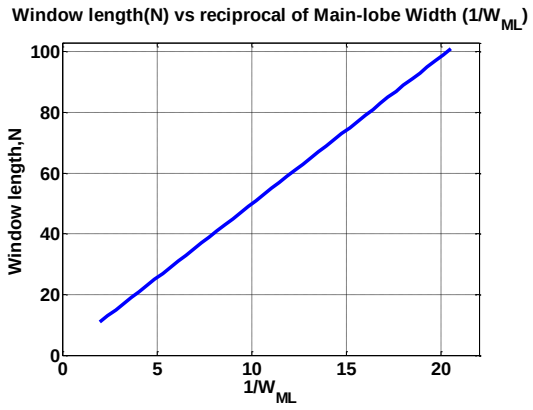

Figure 8. The variation of the N with $1/W_{ML}$ of the proposed Semi-ellipse window

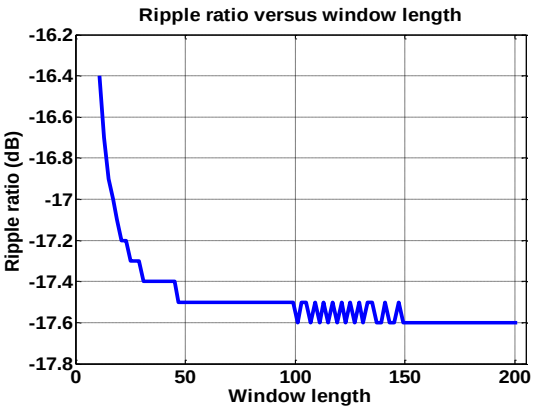

Figure 9. Ripple ratio of the proposed window versus window length

On the other hand, the ripple ratio of the proposed Semi-ellipse window is also plotted as a function of the window length. Figure 9 shows a plot of the numerical results which reveals that the ripple ratio of the proposed window assumes a value of about -17.5 dB which is independent of the window length, N.

The proposed window function is plotted in time domain (see Figure 10) and frequency domain (see Figure 11) using Matlab. The normalized side lobe peak is found to be ≈ -17.5 dB and the normalized main-lobe width is ≈0.098π rad/sample for N = 51. Table 1 shows the window parameters of the proposed Semi-ellipse window put together with the existing fixed windows parameters as presented in [2, 4, 6].

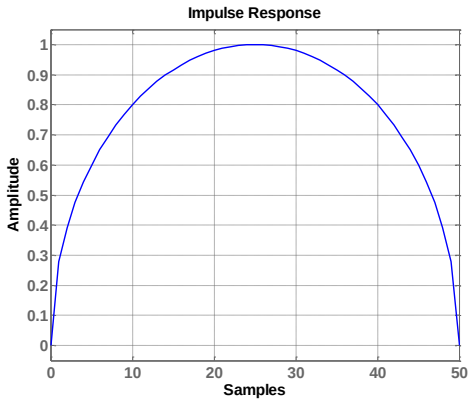

Figure 10. The Semi-ellipse window in the time domain for N = 51

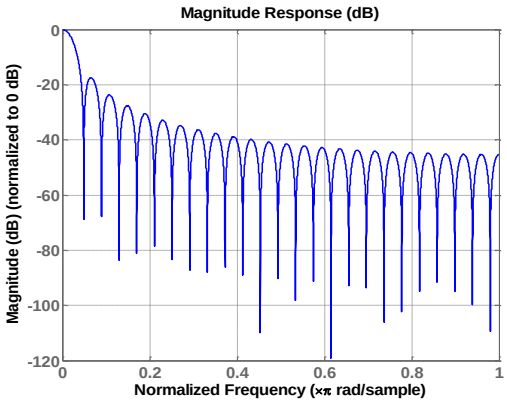

Figure 11. The Semi-ellipse window in the frequency domain for N = 51

Table 1. Window parameter of the proposed Semi-ellipse window with other fixed windows

Window Type	Main-lobe width (xπ rad/sample)	Ripple ratio (dB)
Rectangular	$4/N$	-13.3
Triangular (Bartlett)	$8/N$	-26.5
Von Hann	$8/N$	-31.5
Hamming	$8/N$	-42.3
Blackman	$12/N$	-58.1
Proposed Semi-ellipse	$\mathbf{5/N}$	**-17.5**

2.4. FIR digital filter design using windows

Generally, the filters designed using windows have symmetrical impulse response. In the filter design using window technique, an ideal frequency response of the desired filter is assumed which produces an

infinite duration impulse response upon application of inverse Fourier transform. Practically, ideal filters cannot be implemented, but by approximation practically realizable filters can be achieved. The ideal and realizable frequency response of a lowpass filter as shown in Figure 12 [2] as given by [2-4, 6]:

$$H_{id}(e^{j\omega T}) = \begin{cases} 1\,; & |\omega| \le \omega_c \\ 0\,; & \omega_c < |\omega| \le \pi \end{cases} \quad (26)$$

where ω_c is the cut-off frequency.

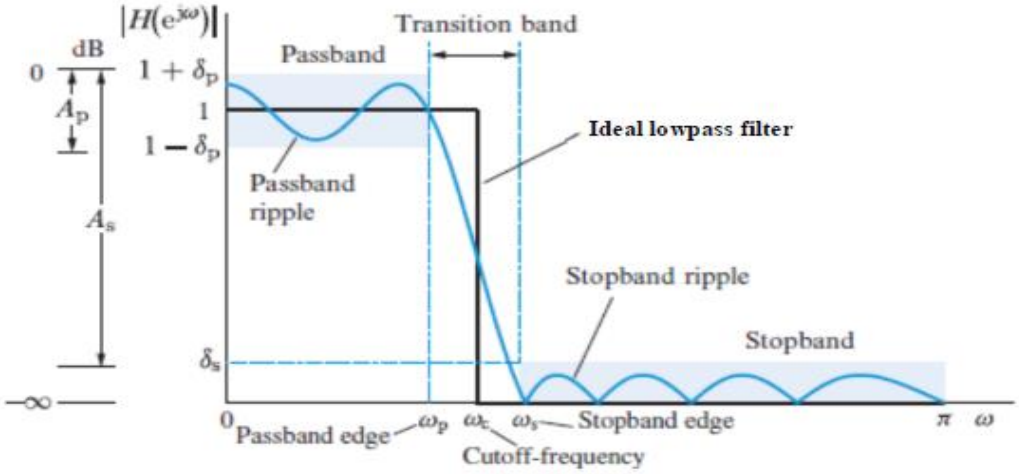

Figure 12. The frequency response of the ideal and realizable lowpass filter

The infinite impulse response of a lowpass filter is as expressed below:

$$h_{id}(nT) = \begin{cases} \frac{sin\omega_c nT}{n\pi}\,; & n \neq 0 \\ \frac{\omega_c}{\pi}; & n = 0 \end{cases} \quad (27)$$

Thus, $-\infty \le n \le \infty$

The impulse response of a realizable finite-duration filter is obtained by multiplying the infinite-duration impulse response, $h_{id}(nT)$ by the window function, $w(nT)$ as in the expression [2-4].

$$h(nT) = h_{id}(nT) * w(nT);\ -M \le n \le M \quad (28)$$

Where $w(nT)$ is a window function of length, N = 2M + 1

If N is odd, then n is an integer and fraction if N is even.
Thus, for odd length: |n| = {0, 1, 2, 3, ….., M} and
for even length: |n| = {0.5, 1.5, 2.5, 3.5, ….., M}

In this paper, N is taken to be odd because odd-length FIR filter is easy and preferred for designing all filter types [2, 18]. The filter realized in (28) in noncausal, and the causal filter can be obtained by delaying the impulse response by a period $(N-1)/2$ as expressed below:

$$h(n) = h\left(\left(n - \left(\frac{N-1}{2}\right)\right)T\right);\ 0 \le n \le N-1 \quad (29)$$

The periodic convolution of the ideal frequency response, $H_{id}(e^{j\omega})$ and the frequency spectrum of the window, $W(e^{j\omega})$ produces the frequency response of the FIR filter, $H(e^{j\omega T})$. This is given by:

$$H(e^{j\omega T}) = H_{id}(e^{j\omega}) \circledast W(e^{j\omega}) = \frac{1}{2\pi}\int_{-\pi}^{\pi} H_{id}\left(e^{j(\omega-\theta)T}\right) W\left(e^{j\theta}\right) d\theta \quad (30)$$

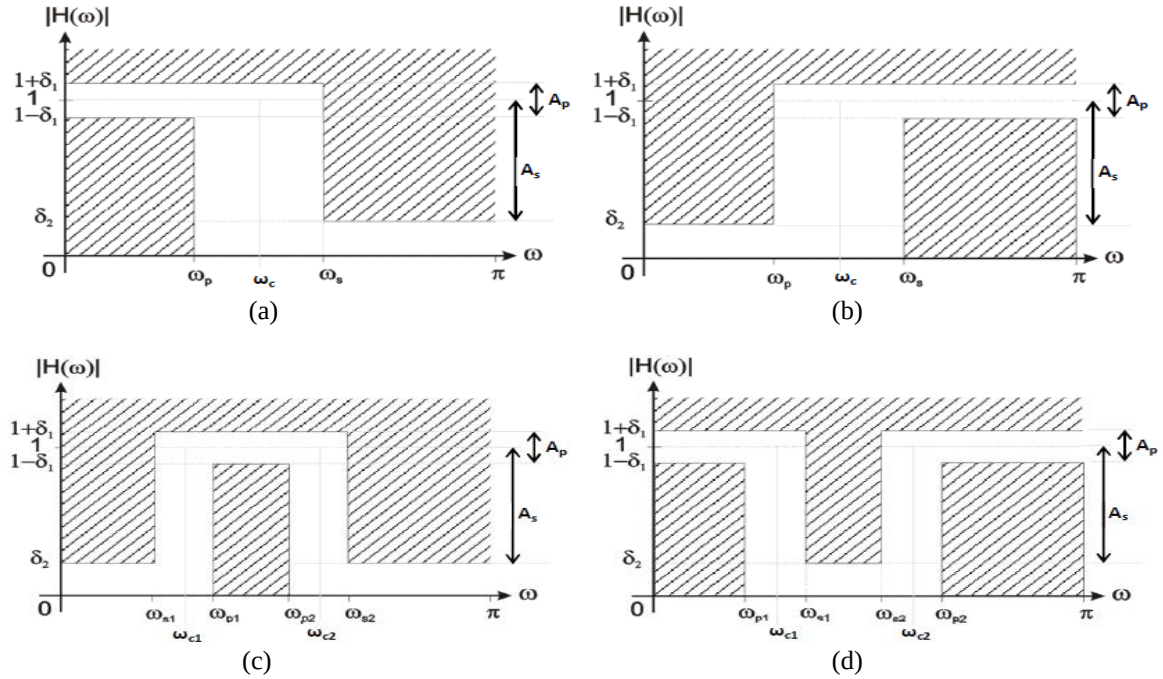

Figure 13. The frequency responses of (a) Lowpass, (b) Highpass (c) Bandpass and (d) Bandstop filters

Although Figure 12 shows the frequency response for a lowpass filter, the relation of the ripples is valid for other filter types as shown in Figure 13[3]. The diagrams show the ideal frequency responses of all the four standard filters and their impulse responses can be computed using their respective functions as shown in Table 2 [3, 19].

Table 2. The causal impulse response of the standard filters {where $M = (N-1)/2$}

Filter Type	Ideal Impulse Response function
Lowpass	$h_{id}(n) = \begin{cases} \frac{\sin(\omega_c(n-M))}{\pi(n-M)}; for\ n \neq M \quad (0 \leq n \leq 2M) \\ \frac{\omega_c}{\pi}; \quad n = M \end{cases}$
Highpass	$h_{id}(n) = \begin{cases} -\frac{\sin(\omega_c(n-M))}{\pi(n-M)}; for\ n \neq M \quad (0 \leq n \leq 2M) \\ 1 - \frac{\omega_c}{\pi}; \quad n = M \end{cases}$
Bandpass	$h_{id}(n) = \begin{cases} \frac{\sin(\omega_{c_2}(n-M))}{\pi(n-M)} - \frac{\sin(\omega_{c_1}(n-M))}{\pi(n-M)}; for\ n \neq M \quad (0 \leq n \leq 2M) \\ \frac{\omega_{c_2}-\omega_{c_1}}{\pi}; \quad n = M \end{cases}$
Bandstop	$h_{id}(n) = \begin{cases} \frac{\sin(\omega_{c_1}(n-M))}{\pi(n-M)} - \frac{\sin(\omega_{c_2}(n-M))}{\pi(n-M)}; for\ n \neq M \quad (0 \leq n \leq 2M) \\ 1 - \frac{\omega_{c_2}-\omega_{c_1}}{\pi}; \quad n = M \end{cases}$

The transition width Δω, the peak-to-peak passband ripple A_p, and the minimum stopband attenuation A_s can be calculated using (31), (32) and (33), respectively for a specified sampling frequency.

$$\Delta\omega = \omega_s - \omega_p \tag{31}$$

$$A_p = 20\log(\frac{1+\delta_p}{1-\delta_p}) \tag{32}$$

$$A_s = -20\log\delta_s \tag{33}$$

Then, set $\delta = min\{\delta_s, \delta_p\}$ (34)

where δ_p is the peak ripple value in the passband, δ_s in the peak ripple value in the stopband, ω_s is the stopband edge frequency, and ω_p is the passband edge frequency.

Therefore, (33) can be rewritten as:

$$A_s = -20\log\delta \tag{35}$$

The transistion bandwidth is symmetric about the cutoff frequency, ω_c; therefore, ω_c can be computed as in the expression:

$$\omega_c = \frac{\Delta\omega}{2} = \frac{\omega_s - \omega_p}{2} \tag{36}$$

The normalized frequency can be determined from the absolute frequency using the expression:

$$\omega = \frac{2\pi f}{f_{samp}} \quad (37)$$

Where f is the absolute frequency in cycle/sec, $f_{samp} = {}^{1}/_{T}$ is the sampling rate in samples/sec, and ω is the normalized frequency in radians/sample

2.4.1. FIR digital filter using the proposed window

In the filter application, the window main-lobe width is responsible for the transition width of the filter while the ripple ratio affects the passband and stopband ripples. Hence, the narrower the main-lobe width, the better the transition width and the smaller the ripple ratio the better the passband ripple and stopband attenuation. However, narrower transition width and smaller ripples are desired in filter applications, but windows trade-off main-lobe width with maximum side-lobe amplitude therefore reduction of both quantities cannot be achieved at the same time.

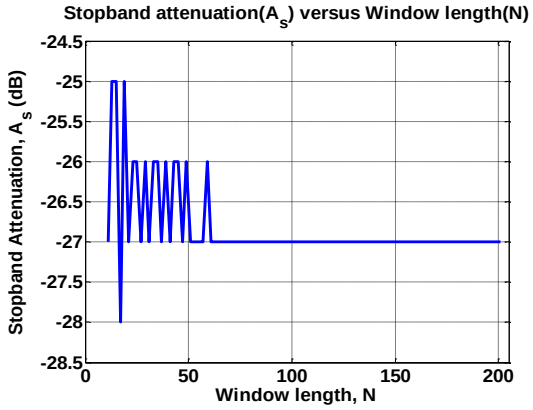

Figure 14. Stopband attenuation of the proposed window versus window length

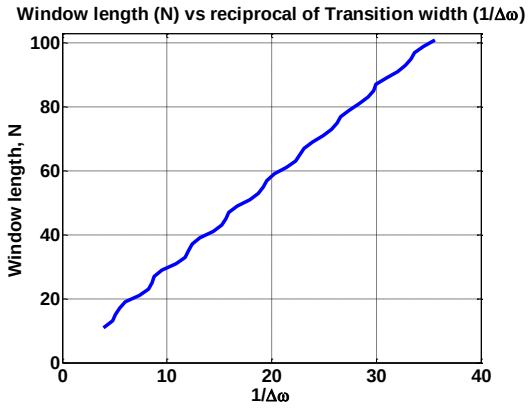

Figure 15. Filter length versus the reciprocal of the transition width of the proposed window

Furthermore, to determining the parameters of the proposed window in filter application, we used the proposed window in a lowpass filter design due to the fact that other filters are designed using lowpass filter and then transforming it to the desired response [4, 20]. The frequency spectrum of the proposed window in a lowpass filter is determined using (30) and stopband attenuation is plotted as a function of the filter length as shown in Figure 14. This simulation can be done easily in Matlab [2, 6, 19, 21, 22]. The simulation results presented in Figure 14 shows that as we increase the window length N, the stopband attenuation of the proposed Semi-ellipse is approximately -27 dB which is independent of the filter length like in the case of the ripple ratio (see Figure 9). As shown previously in Figure 8, the transition width, Δω also decreases as the filter length increases; thus, $N \propto 1/\Delta\omega$. A plot of N versus 1/Δω for the proposed window is shown in Figure 15. The result shows that the estimated transition width of the proposed window in FIR filter design can be determined as in (38). Table 3 [2, 6, 19] shows the summary of the parameters of the popular fixed window functions with the proposed window parameters added in bold letters at the bottom of the table.

$$\Delta\omega_{se} \approx \frac{2.8}{N} \ (\text{x}\pi \text{ rad/sample}) \quad (38)$$

where $\Delta\omega_{se}$ is the proposed Semi-ellipse transition width and N in the filter length

Table 3. Window parameter of the proposed Semi-ellipse window with other fixed windows

Window Name	Transition width, $\Delta\omega$ (xπ rad/sample)		Min. Stopband Attenuation
	Approximate value	Exact value	(dB)
Rectangular	${}^{4}/_{N}$	${}^{1.8}/_{N}$	21
Triangular (Bartlett)	${}^{8}/_{N}$	${}^{6.1}/_{N}$	26
Von Hann	${}^{8}/_{N}$	${}^{6.2}/_{N}$	44
Hamming	${}^{8}/_{N}$	${}^{6.6}/_{N}$	53
Blackman	${}^{12}/_{N}$	${}^{11}/_{N}$	74
Proposed Semi-ellipse	$\mathbf{{}^{5}/_{N}}$	$\mathbf{{}^{2.8}/_{N}}$	**27**

In the design of nonrecursive filters using fixed windows, the minimum stopband attenuation is determined to confirm the window is suitable for designing the prescribed filter. The choice of the minimum stopband attenuation is selected such that it is a little greater than that of the prescribed filter. A lowpass filter can be designed using the proposed Semi-ellipse window by applying some equations expressed in the previous sections in this paper. First of all, the minimum stopband attenuation of the prescribed filter is determined as in (32 - 35) using the given filter design specifications. Assuming A_s of the proposed window satisfies the filter specification presented, the algorithm shown below can be used to design a lowpass FIR filter using the proposed Semi-ellipse window.

Algorithm for lowpass filter design using Semi-ellipse window:

Step 1. Input the filter specification ω_s, ω_p, A_s and A_p.

Step 2. Compute the transition width, $\Delta\omega$ of the filter using (31).

Step 3. Compute ω_c using (36).

Step 4. Compute the filter length, N required for the specified transition width using (38) and rounding up to the nearest odd integer.

Step 5. Compute the window function coefficients using (18) or (24) according to the filter length obtained in Step 4.

Step 6. Compute the ideal lowpass filter impulse response coefficients as in Table 2 according to the filter length obtained in Step 4.

Step 7. Compute the causal finite-duration impulse filter as in (29)

Step 8. Check the filter design achieved to ensure it satisfies the prescribed specification, and if it does not, increase N by 2 and go back to Step 5.

The Algorithm for the design of lowpass filter can also be used in the design of highpass, bandstop and bandpass filter. However, for bandstop and bandpass filters, the narrower of the two transition bandwith is selected for the filter design [2, 4]. Therefore,

For bandstop: $\Delta\omega = \min\left[\left(\omega_{s_1} - \omega_{p_1}\right), \left(\omega_{p_2} - \omega_{s_2}\right)\right]$ (39)

and $\omega_{c_1} = \omega_{p_1} + \frac{\Delta\omega}{2}$ and $\omega_{c_2} = \omega_{p_2} - \frac{\Delta\omega}{2}$

For bandpass: $\Delta\omega = \min\left[\left(\omega_{p_1} - \omega_{s_1}\right), \left(\omega_{s_2} - \omega_{p_2}\right)\right]$ (40)

and $\omega_{c_1} = \omega_{p_1} - \frac{\Delta\omega}{2}$ and $\omega_{c_2} = \omega_{p_2} + \frac{\Delta\omega}{2}$

Example 1

Design a lowpass filter with the following specifications: $f_p = 5\ kHz$, $f_s = 5.6\ kHz$, $\delta = 0.056$ and $f_{samp} = 25\ kHz$ using the Triangular (Bartlett), Hann, Hamming, Kaiser and Semi-ellipse windows.

Solution:

Step 1. Using (35), $A_s \approx 25\ dB$.

Step 2. Using (37), $\omega_p = 0.4\pi$ *and* $\omega_s = 0.448\pi\ (rad/sample)$
Using (31), $\Delta\omega = 0.048\pi$ (rad/sample).

Step 3. Using (36), compute ω_c of the ideal filter as $\omega_c = 0.424\pi\ (rad/sample)$.

Step 4. From Table 3, the filter lengths that will satisfy the transition width for Bartlett, Hann, Hamming, and Semi-ellipse were determined as N = 127, 129, 137, and 59, respectively.
Using (8) and (7), the Kaiser parameters N and β were determined as 51 and 1.332, respectively

Step 5. Compute the window function coefficients for the Triangular as in (2), Hann as in (3), Hamming as in (4), Kaiser as in (6) and Semi-ellipse as in (18) using their filter lengths obtained in Step 4.

Step 6. Compute the ideal lowpass filter impulse response coefficients as in Table 2 using the filter lengths obtained in Step 4.

Step 7. Compute the causal finite-duration impulse reponse using results of Step 5 and Step 6 for the windows.

Step 8. The parameters obtained were used in Matlab to plot the frequency response of the filter using the different windows. The minimum stopband attenuation obtained for Bartlett, Hann, Hamming, Kaiser, and Semi-ellipse were -26.30, -44.00, 53.40, -25.99, and -27.15 dB; the

transistion widths achieved were 0.0502π, 0.0488π, 0.0493π, 0.0485π, 0.048π rad/sample, respectively. Figure 16 shows the magnitude responses of the designed lowpass filters.

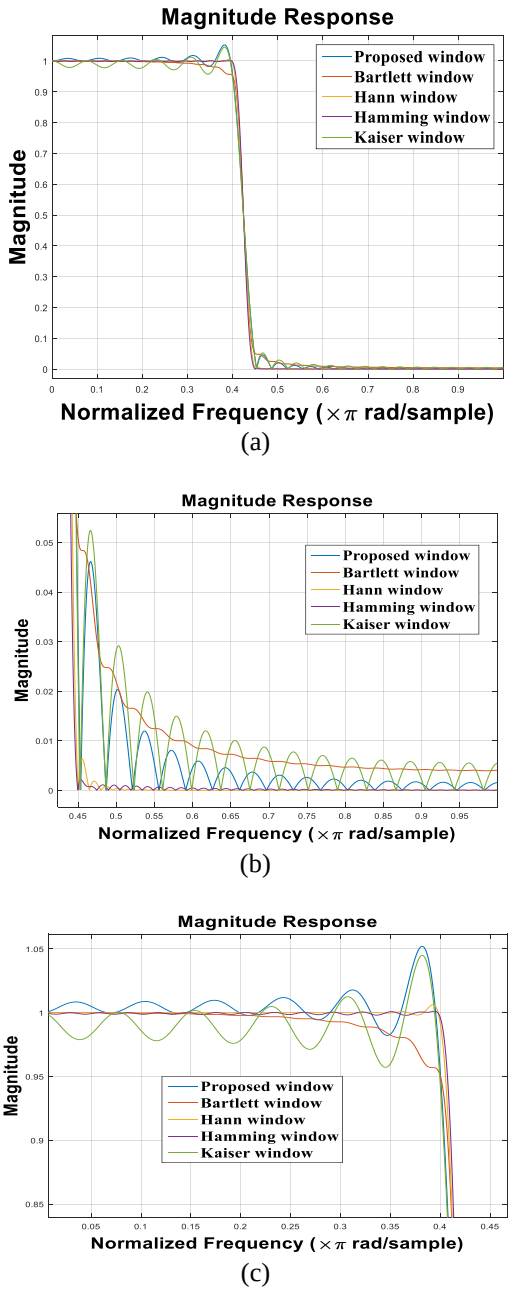

Figure 16. Diagram shows (a) the frequency response of the lowpass filters of Example 1, an enlarged view of the (b) stopband and (c) passband ripples

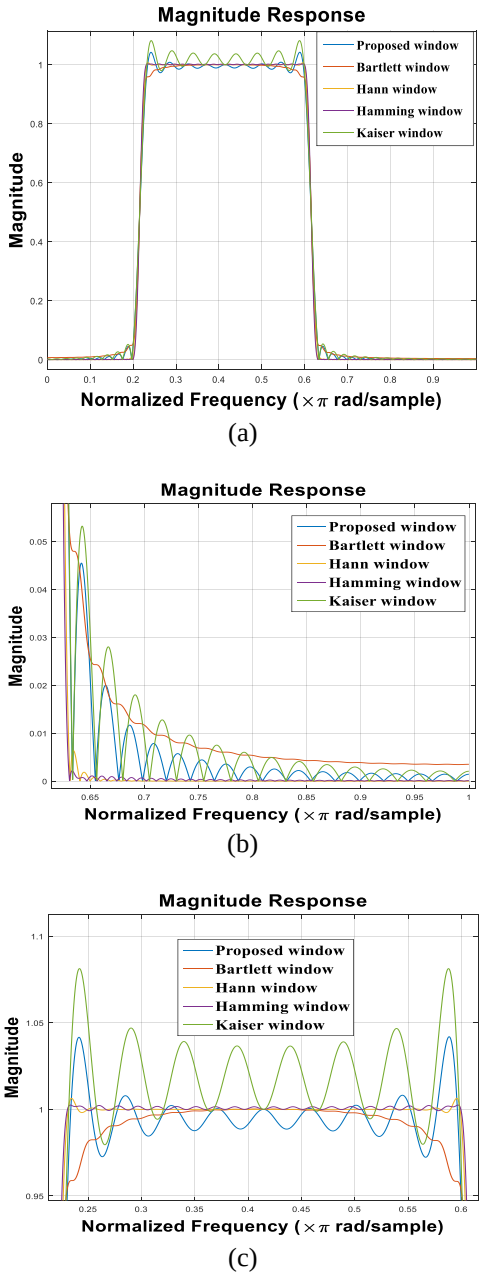

Figure 17. Diagram shows (a) the frequency response of the bandpass filters of Example 2, an enlarged view of the (b) stopband and (c) passband ripples

Example 2

Design a bandpass filter with the specifications below using the Triangular (Bartlett), Hann, Hamming, Kaiser and Semi-ellipse windows. For $0 \leq \omega \leq 100$: $A_s = 25.0\ dB$

For $115 \leq \omega \leq 300$: $A_p = 1.0\ dB$

For $325 \leq \omega \leq 500$: $A_s = 25.0\ dB$

$f_{samp} = 1000\ Hz$

Solution:

Step 1. Using (32) and (33), $\delta_p = 0.0575$ and $\delta_s = 0.0562$ and using (35), $A_s = 25.0\ dB$

Step 2. Using (37), $\omega_{s_1} = 0.2\pi$, $\omega_{p_1} = 0.23\pi$, $\omega_{p_2} = 0.6\pi$, and $\omega_{s_2} = 0.65\pi\ (rad/sample)$
Using (40), $\Delta\omega = \min(0.03\pi, 0.05\pi) = 0.03\pi$ (rad/sample)

Step 3. Using (40), determine ω_{c_1} and ω_{c_2} of the ideal passband filter as $\omega_{c_1} = 0.215\pi$ and $\omega_{c_2} = 0.615\pi\ (rad/sample)$

Step 4. From Table 3, the filter lengths that will satisfy the transition width for Bartlett, Hann, Hamming, and Semi-ellipse were determined as N = 203, 207, 221, and 93, respectively.
Using (8) and (7), the Kaiser parameters N and β were determined as 81 and 1.332, respectively

Step 5. Like in Example 1, the window function coefficients for the Triangular, Hann, Hamming, Kaiser and Semi-ellipse window were determined using the filter lengths obtained in Step 4.

Step 6. Compute the ideal bandpass filter impulse response coefficients as in Table 2 using the filter lengths obtained in Step 4.

Step 7. Compute the causal finite-duration impulse reponse using results of Step 5 and Step 6 for the different windows.

Step 8. The parameters obtained were used in Matlab to plot the frequency response of the filter using the different windows. The minimum stopband attenuation obtained for Bartlett, Hann, Hamming, Kaiser, and Semi-ellipse were -26.29, -43.94, 53.25, -25.75, and -27.03 dB; the transistion widths achieved were 0.0302π, 0.0304π, 0.0300π, 0.0281π, 0.0314π rad/sample, respectively. Figure 17 shows the magnitude responses of the designed bandpass filters.

3. RESULTS AND DISCUSSION

The experiments to determine the proposed window parameter in Figure 8 and 9 show that its main-lobe width is about $^{5\pi}/_{N}$ rad/sample and its ripple ratio remains relatively independent of N at approximately -17.5 dB for values of N in the range 11 to 201. In filter design, its minimum stopband attenuation also remains relatively independent of N at approximately 27 dB for values of N in the range 11 to 201(see Figure 14) while Figure 15 reveals that its transition width is about $^{2.8\pi}/_{N}$ rad/sample.

Table 4. Summary of results of Examples 1 and 2

Window Name	Filter Length, N	Transition Width, Δω (Rad/sample)	Minimum Stopband Attenuation, A_s (dB)
	Results of Example 1 – Lowpass filter		
Triangular (Bartlett)	127	0.0502	26.30
Von Hann	129	0.0488	44.00
Hamming	137	0.0493	53.40
Kaiser (β = 1.332)	51	0.0485	25.99
Proposed Semi-ellipse	59	0.0480	27.15
	Results of Example 2 – Bandpass filter		
Triangular (Bartlett)	203	0.0302	26.29
Von Hann	207	0.0304	43.94
Hamming	221	0.0300	53.25
Kaiser (β = 1.332)	81	0.0281	25.75
Proposed Semi-ellipse	93	0.0314	27.03

In the two filter application examples illustrated in this paper, the fixed windows Triangular (Bartlett), Hann, Hamming, proposed window and the adjustable Kaiser window satisfy the requirements for the two filter specifications presented. Table 4 summarizes the numerical results of the lowpass and bandpass filters of Example 1 and 2, respectively. The filters designed for the lowpass and bandpass filters using the windows are shown in Figures 16 and 17, respectively. As observered in Figure 16(a) and 17(a), the transition widths of all the filters implemented with the different windows closely approximates the specified transition widths in both examples as recorded in Table 4.

In both examples presented in this paper, it is observed from Table 4 that the Hamming and Von Hann windows produced the best minimum stopband attenuation of 53 dB and 44 dB, respectively, which is far more than the minimum stopband attenuation (25 dB) of the prescribed filter. The choice of the Hamming and Hann windows with minimum stopband attenuation far greater than the prescribed filter, as expected, produced a trade-off in the transition width which can only be compensated with increase in the number of

coefficients (filter length). This in turn increases the filter complexity which is not desired in FIR filter design. As observed in Table 4, the number of coefficients required to implement the filters using Hamming and Hann windows in both Examples (137 and 129, respectively, in the lowpass-filter example, and 221 and 207, respectively, in the bandpass-filter example) are more than twice the number of coefficients used to implement the same filters for the Kaiser window and the proposed window. Besides, the filters implemented with both windows produced minimal ripples in the passband and stopband compared to the other filters implemented with the other windows in this study.

In the other hand, the Bartlett window (A_s = 26 dB) is just right for the stopband attenuation presented (25 dB), but the filter lengths required to satisfy the filters (127 in Example 1, and 203 in Example 2) in both Examples are more than twice that are needed in the case of Kaiser and the proposed window like in the case of the Hamming and Von Hann windows.

The adjustable Kaiser window ($A_s \approx 26$ dB), which can be tuned with its independent parameter β to satisfy the prescribed filters in both Examples, implements the filters with the least filter lengths (51 for the lowpass filter, and 81 for the bandpass filter).

The proposed window (A_s = 27 dB) implements the filters in both cases with minimal filter lengths (59 and 93 for the lowpass and bandpass filters, respectively) than the other fixed windows which implies reduction in filter complexity. Although the Kaiser window produced a little fewer coefficients filters than the proposed window compared to the Hann, Hamming and Bartlett windows used in the Examples, the proposed window produced smaller ripples along the stopband and passband than the Kaiser window (see part (b) and (c) of Figures 16 and 17).

4. CONCLUSION

In this paper, a new fixed elliptical window which is derived from the equation of an ellipse is proposed. Its main-lobe width is about $5\pi/N$ rad/sample and its ripple ratio is about -17.5 dB which remains relatively independent of the filter length. In filter design, its minimum stopband attenuation also remains relatively independent of the filter length at approximately 27 dB while the transition width is about $2.8\pi/N$ rad/sample. In the investigation of the proposed window in filter design, the performance was proven to be better than the Bartlett window in terms of stopband attenuation and filter length where it can be used to design better filters using less than half the Bartlett's filter length for a fixed transition width. The proposed window produced smaller amplitude ripples along the passband and stopband than the Kaiser while the Kaiser used fewer coefficients for a fixed transition width. Besides, the simplicity in the proposed window's coefficients formulation and design algorithm may make it preferable to the Kaiser window.

In this paper, we introduced a new fixed window - the Semi-ellipse window. We studied its spectral characteristic and its filter applications illustrated with some examples confirmed that its performance can be compared with other standard fixed windows. However, window function is selected based on the one that best satisfies the filter specification presented. The combination of the proposed window with other windows, like in the case of Bartlett-Hann window, will in no doubt produce filters with better filtering characteristics. This set a direction for further research.

REFERENCES

[1] A. Autoniou, "Digital filters," in Digital Signal Processing - Signals, Systems and Filters, 1st ed. New York, USA: McGraw-Hill, pp. 19-28, 2005.
[2] D. Manolakis and V. Ingle, "Design of FIR Filters," in Applied Digital Signal Processing - Theory and Practice, 1st ed. New York, USA: Cambridge University Press, pp. 537-623, 2011.
[3] M. Zoran, "Window Functions" in Digital Filter Design, MikroElektronika, 2009, [Online]. Available: https://www.mikroe.com/ebooks/digital-filter-design/window-functions
[4] A. Autoniou, "Design of Nonrecursive (FIR) Filters," in Digital Signal Processing - Signals, Systems and Filters, 1st ed. New York, USA: McGraw-Hill, pp. 425-462, 2005.
[5] S. W. Smith, "Gibbs effect," in The Scientist and Engineer's Guide to Digital Signal Processing, 2nd ed. San Diego, California, USA: California Technical Publishing, pp. 218-219, 1999.
[6] V. K. Ingle and J. G. Proakis, "FIR Filter Design," in Digital Signal Processing using Matlab:. 3rd ed. Stamford, USA: Cengage Learning, pp. 303 -375, 2012.
[7] A. W. Doerry, "Catalog of Window Taper Functions for Sidelobe Control", California, USA: Sandia National Laboratories, pp. 39-194, 2017. [Online]. Avaliable: https://prod-ng.sandia.gov/techlib-noauth/access-control.cgi/2017/174042.pdf
[8] T. Saramäki, "Finite Impulse Response Filter Design," in Handbook for Digital Signal Processing, S. K. Mitra and J. F. Kaiser, Eds.,Wiley & Sons, New York, NY, USA, 1993.

[9] J. F. Kaiser, "Nonrecursive Digital Filter Design using the I0-sinh Window Function," Proceedings / IEEE International Symposium Circuits and Systems, pp. 20–23, April 1974.
[10] S. W. A. Bergen and A. Antoniou, "Design of Nonrecursive Digital Filters using the Ultraspherical Window Function. Eurasip Jornal on Advanced Signal Processing, vol 12, pp. 1910-1922, 2005.
[11] C. L. Dolph, "A Current Distribution for Broadside Arrays Which Optimizes the Relationship between Beamwidth and Side-Lobe Level," Proceedings of the IRE, vol. 34, pp. 335–348, June 1946.
[12] F. J. Harris, "On the Use of Windows for Harmonic Analysis with the Discrete Fourier Transform," Proceedings of the IEEE, Vol. 66, No. 1, pp. 51-83, January 1978.
[13] E. Jaya, K.C. Rao and J.L. Anem, "FIR Filter Design using New Hybrid Window Functions," International Journal of Science, Engineering and Technology Research (IJSETR), Vol. 4, Issue 6, pp. 1793 – 1797, June 2015.
[14] H. Rakshit and M. A. Ullah , "FIR Filter Design using an Adjustable Novel Window and its Applications," International Journal of Engineering and Technology (IJET), Vol. 7, No. 4, August 2015, pp. 1151-1162.
[15] T. Karmaker, M. S. Anower, M. A. G. Khan and M. A. Habib, "A New Adjustable Window Function to Design FIR Filter and its Application in Noise Reduction from Contaminated ECG Signal" 2017 IEEE Region 10 Humanitarian Technology Conference (R10-HTC), Dhaka, Bangladesh, December 2017.
[16] S. W. A. Bergen and A. Antoniou, "Design of Ultraspherical Window Functions with Prescribed Spectral Characteristics," Applied Journal of Signal Processing, vol. 13, pp. 2053–2065, 2004.
[17] J. D. Page, "General equation of an ellipse" (2011), Retrieved February 22, 2019, from Math Open Reference, https://www.mathopenref.com/coordgeneralellipse.html
[18] A. Autoniou, "The Discrete Fourier Transform," in Digital Signal Processing - Signals, Systems and Filters, 1st ed. New York, USA: McGraw-Hill, pp. 321-388, 2005.
[19] L. Tan and J. Lean , "Finite Impulse Response Filter Design," in Digital Signal Processing Fundamentals and Applications", 2nd ed., MA, USA : Elsevier Inc., pp. 217-299, 2013.
[20] S. W. Smith, "Introduction to Digital Filters," in The Scientist and Engineer's Guide to Digital Signal Processing, 2nd ed. San Diego, California, USA: California Technical Publishing, pp. 261-276, 1999.
[21] W. Y. Yang, T. G. Chang, Ik H. Song, Y. S., Cho, j. Heo. W. G. Jeon, J. W. Lee and J. K. Kim, "Analog and Digital Filters," in Signals and System with Matlab, 1st ed. Heidelberg, Germany: Springer, pp. 307-360, 2009.
[22] J. W. Leis, "Discrete-Time Filters," in Digital Signal Processing using Matlab for Students and Researchers, 1st ed. New Jersey, USA: John Wiley & Sons, Inc., pp. 271-314, 2011.

BIOGRAPHY OF AUTHORS

Uzo Henry N. is a chief engineer in Scientific Equipment Development Institute (SEDI), Enugu-Nigeria. He obtained his B. Eng in Electrical and Electronic Engineering from Enugu State University of Science and Technology, Enugu-Nigeria, and M. Eng in Digital Electronics and Computers in University of Nigeria, Nsukka – Nigeria. Currently, he is a postgraduate researcher at the Department of Electronic Engineering, University of Nigeria Nsukka-Nigeria. E-mail: nhenryuzo@gmail.com

Oparaku Ogbonna U. obtained a Bachelor of Engineering degree in Electrical /Electronic Engineering in 1980 and a PhD in 1988 from the University of Northumbria at Newcastle-Upon-Tyne, United Kingdom. He has lectured and done extensive research within University of Nigeria since 1988 in collaboration with other institutions. He served as the Director of the National Centre for Energy Research and Development from 2004-2009, Head, Department of Electronic Engineering from 2011-2014 and Dean, Faculty of Engineering from 2016-2018. His specific areas of research are Digital Electronics and Solid State Electronics. Email: ogbonna.oparaku@unn.edu.ng

Chijindu Vincent C. is a Senior Lecturer at the Department of Electronic Engineering, University of Nigeria, Nsukka, Nigeria. He obtained B.Eng and M.Eng in Electronic and Computer Engineering from Anambra State University of Technology Enugu Nigeria and Ph.D. in Computer and Control Engineering from Nnamdi Azikiwe University Awka Nigeria. His current research interests include artificial intelligence in medical diagnosis, digital signal/image processing, renewable energy systems and wireless sensor networks. E-mail: vincent.chijindu@unn.edu.ng